Mineralogy, geochemistry, and reserve estimation of the Euphrates limestone for Portland cement industry at Al-Najaf area, South Iraq

Mautaz Al-Dabbas, Salih Muhammad Awadh & Ayad Abed Zaid

Arabian Journal of Geosciences

ISSN 1866-7511
Volume 6
Number 2

Arab J Geosci (2013) 6:491-503
DOI 10.1007/s12517-011-0370-z

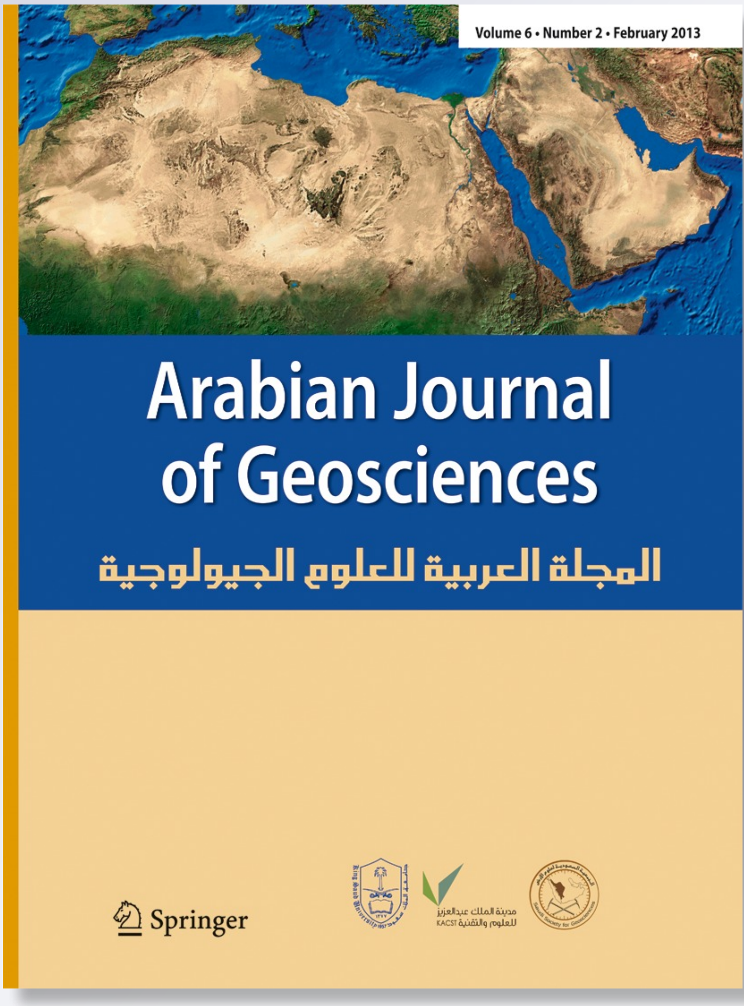

Springer

Arab J Geosci (2013) 6:491–503
DOI 10.1007/s12517-011-0370-z

ORIGINAL PAPER

Mineralogy, geochemistry, and reserve estimation of the Euphrates limestone for Portland cement industry at Al-Najaf area, South Iraq

Mautaz Al-Dabbas · Salih Muhammad Awadh · Ayad Abed Zaid

Received: 12 April 2011 / Accepted: 20 June 2011 / Published online: 7 July 2011

Abstract This study deals with the mineralogical and geochemistry of the Euphrates Formation (Lower Miocene) in Bahr Al-Najaf area in order to assess the lithofacies of the Euphrates Formation for Portland cement manufacturing. Petrographic and mineralogical studies were carried out on 210 core samples, collected from 21 boreholes, and showed that calcite is the dominant mineral with few amounts of quartz, gypsum, feldspar, and a rare amount of dolomite. Clay mineral suites (palygorskite, kaolinite, montmorillonite, and illite) formed about 5% from the total mineral composition. Palygorskite precipitated directly in alkali shallow water rich with Si and Mg ions. Chemical weathering of feldspar under acidic conditions participated in formation of Kaolinite. Geochemistry showed that there is no high variation in chemical constituents with depth, and the average of CaO (51.5), MgO (0.83), SO_3 (0.54), SiO_2 (4.3), Fe_2O_3 (0.45), Al_2O_3 (0.93), L.O.I (40.7), Na_2O_3 (0.08), K_2O (0.14), and Cl^- (0.1) qualified the lithofacies of Euphrates Formation to be raw materials suitable for manufacturing the Portland cement. Triangle Block method is applied to estimate the reserve on square area (2×2 km^2) which is computed to be 63 million tons of medium-tough limestone as potential probable reserve.

Keywords Mineralogy · Geochemistry · Reserve estimation · Cement industry · Iraq

M. Al-Dabbas · S. M. Awadh (✉)
Earth Sciences Department, College of Science,
University of Baghdad,
Baghdad, Iraq
e-mail: salihauad2000@yahoo.com

A. A. Zaid
Al-Kufa Cement Plant,
Kufa, Iraq

Introduction

The cement production in Iraq was initiated at 1949, where the first plant was established with production capacity of about 8,000 t per year. As a result of economic and constructional progress and project development, there was an increase in demand of this material and to serve new companies and plants to cover local market needs. The General Southern Company for Cement is one of three companies that were distributed to in the north, central, and south of Iraq. This includes eight factories in: Al-Najaf, Al-Kufa, Karbala, Al-Sadaa, Al-Muthana, Al-Samawa, and Um-Qasir. Their conventional products are two kinds of cement, normal and resistance. Industrialization of these products depended on raw materials such as limestone, clay, and gypsum, which were considered as the key to success of the cement industry. The favorable formation for purpose of Portland cement industry is the Euphrates Formation.

The chemical composition for the clinker of Portland cement (mixture from 70% limestone+30% clay) depends essentially on the chemical composition of the raw materials (Dabous et al. 1989).

The Euphrates Formation which has many exposures in the Iraqi Western Desert especially along the Euphrates River and in the south of Iraq, near Al-Najaf, had been deposited in shallow marine environment (Cytroky and Karim 1969, unpublished; Youkhanna 1971, unpublished).

This work aims to assess limestone rocks of the Euphrates Formation based on their geochemical characteristics as cement raw material and to estimate probable reserve.

Location and nature of the study area

Bahr Al-Najaf area is located within the tectonic Salman Zone (Fig. 1) which belongs to the stable shelf zone that is distinct by its shallow Basement Rocks (Jassim and Goff 2006). The area of study is 4,000 km^2 which is accurately determined by the longitudes (44º00′00″–44º30′00″) and latitudes (31º30′00″–32º00′00″). It is situated on the southern west edge of Bahr Al-Najaf. The Euphrates Formation is exposed at the surface of the study area where 21 wells were drilled in (Fig. 1). The elevation and total depth of each well are listed in Table 1.

General geology

The highest point at the study area has an altitude of 135 m above the sea level at the northwest, and gradually, land decreases to a minimum (50 m) above the sea level to the

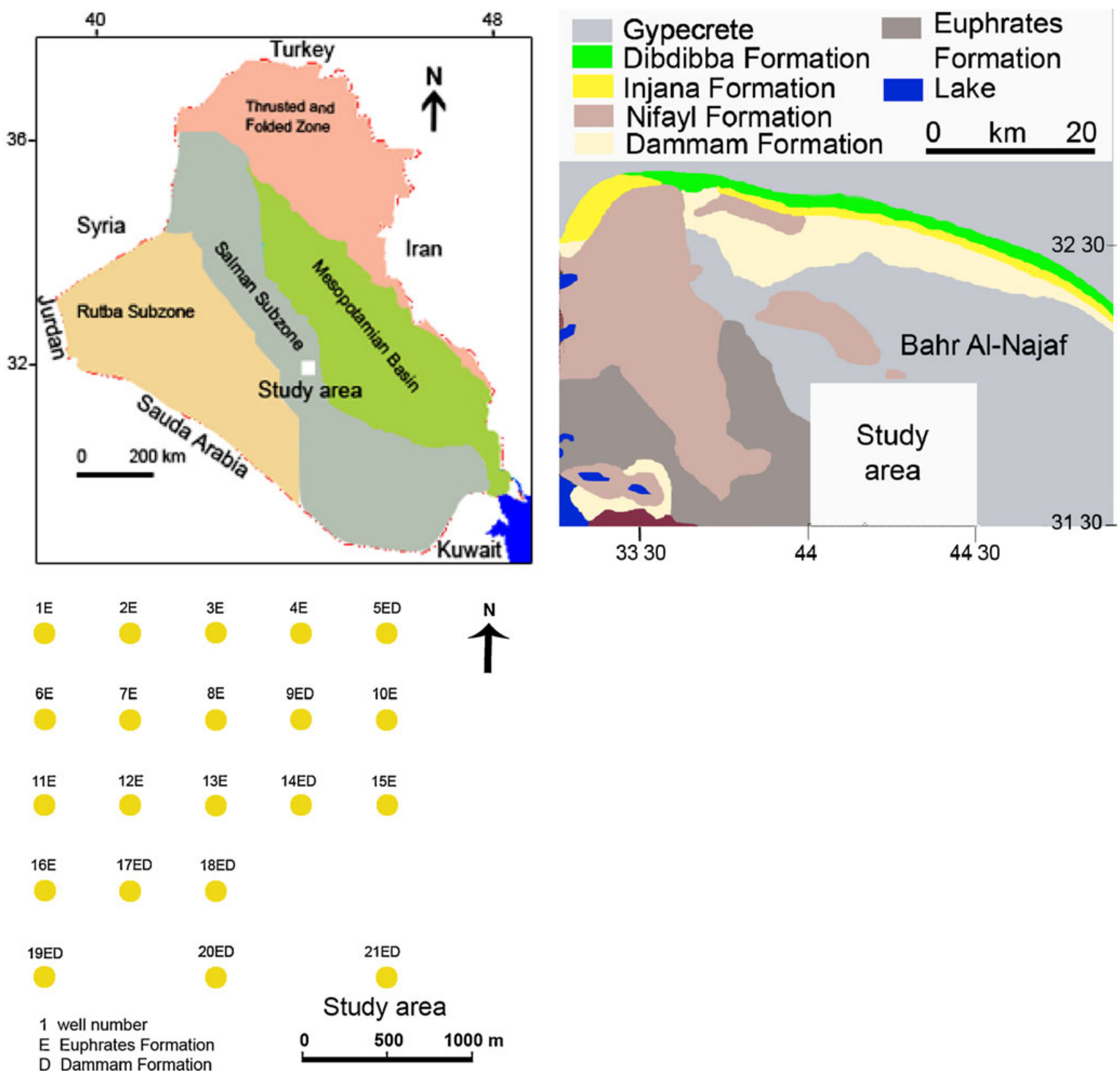

Fig. 1 Simplified tectonic and geological map show the location of study area and borehole grid distribution

Table 1 The elevations and the total depth of wells

Well number	Elevation (m)	Total depth (m)	Well number	Elevation (m)	Total depth (m)
1E	69.0	10	12E	62.30	10
2E	61.3	10	13E	62.80	10
3E	57.0	10	14ED	57.2	10
4E	52.8	10	15E	63.0	10
5ED	56.0	15	16E	65.40	10
6E	64.1	10	17ED	60.0	10
7E	61.0	10	18ED	56.0	10
8E	58.6	10	19ED	66.0	15
9ED	53.48	10	20ED	63.0	10
10E	52.20	10	21ED	72.0	15
11E	70.0	10			

E Ephrates Formation, *D* Dammam Formation

west and southeast. Two main aquifers occur in the study area; the first is represented by recent water-bearing sediments, but the second one is Miocene water-bearing complex (Hassan 1973, unpublished).

Lithostratigraphy could be described from oldest to youngest as Al-Dammam, Euphrates, Nifayl (Fatha), Injana, and Dibdibba Formations, as well as the Quaternary deposits. Al-Dammam Formation consists of recrystallized limestone which contains neritic marine Nummulite and large Foraminifera (Al-Hashimi 1973) belonging to the Middle Eocene. Lateral variation representing the geographic distribution indicates presence of various lithology (thick layers of well stratified limestone, dolomitic limestone, marl, thin layers of chalky limestone, shale, and flint; Buday 1980; Barwary and Naseira 1995), but the vertical variation which represents the deposition time tends to be limited.

Euphrates Formation (Lower Miocene) is composed of dolomitic, fossiliferous, and oolitic limestones with green marls at the top (Al-Hashimi and Amer 1985). It unconformably overlies the Al-Dammam Formation where the basal conglomerates separate between the Euphrates and Dammam formations (Jassim and Goff 2006). Pelecypods, Gastropoda, and Ostracods are present (Cytroky and Karim 1971). Formation in general is divided into three units from bottom to top: cavernous and conglomeratic limestone, marly limestone, and chalky limestone (Buday 1980). The lower and middle units as well as pure limestone are found in the study area.

Fatha (Nifayl) Formation (Middle Miocene) in the north of Iraq is mainly consisted of gypsum, but this lithofacies has been changed into carbonate and marl of shallow marine water (Sissakian 1999). Then, later, it was named Nifayl, which is exposed near the study area, composing of siltstone, green marlstone, and sandstone. The upper contact is conformable with the Injana Formation.

Injana Formation (Upper Miocene-Pliocene; Al-Sayyab et al. 1982) is exposed to the north and northeast of the study area (Fig. 1) with thickness of 27 m composing, in general, a sequence of clay stone, siltstone, and sandstone with silt layers of chalky limestone, and then is reduced toward southeast to 9 m (Dawood 2000**)**. The depositional environment seems to be variable between lagoon at the beginning, riverine and fluvio-lacustrine system.

Dibdibba Formation (Pliocene–Pleistocene) comprises of siltstone, sandstone, little claystone, gravel, pebbles of igneous rocks (in**c**luding pink granite), and white quartz. It is situated unconformably on the Injana Formation (Fig. 1). The formation was deposited in a fresh water environment which becomes deltaic to the NE. The formation is often covered recently by sand sheets or by the alluvial fan sands (Jassim and Goff 2006).

Quaternary deposits which are mainly Aeolian sediments cover the most parts of the study area. Gypcrete deposits consist of friable sands mixed with secondary gypsum (Al-Atia 2001).

Materials and methods

In the study area which is a square shape (2×2 km^2), twenty-one wells were drilled with depth ranges from 10 to 15 m penetrating the Euphrates Formation. Drilling interval is 500 m except the wells 19ED, 20ED, and 21ED which have a 1,000-m interval (Fig. 1). Ten core samples of the Euphrates Formation from each well are collected, then grinded well and mixed together to be a homogenous representative sample. Each sample is analyzed for CaO, MgO, SO_3, SiO_2, Fe_2O_3, Al_2O_3, Na_2O, K2O, Cl^-, and loss on ignition (LOI). Calcium and magnesium were determined by titration against EDTA; Na_2O and K_2O are determined by flame photometry; chloride is determined by titration against $AgNO_3$; silica, alumina, and total iron are determined by using atomic absorption spectrophotometry. LOI is determined by calcinations at 1,100°C for 2 h.

X-ray diffraction (XRD) is used for mineral identification, where velocity of recorder is 4°/s, current is 30 mA, voltage is 40 kV, automatic slit, cupper radiation, and nickel filter. In terms of non-carbonate fraction test, HCl (10%) and CH_3COOH

(5%) added to bulk carbonate samples to remove carbonates; then clay minerals, feldspar, and quartz are identified easily by using XRD. Bulk density and compressive strength are tested in ten core samples collected from ten selected wells. All procedures above are achieved at the State Company of Geological Survey and Mining in Baghdad. For reserve estimation, the Triangle Blocks method is applied.

Results and discussion

Mineralogy

Non-clay minerals are represented by calcite, dolomite, quartz, feldspar, and gypsum, where calcite appears to be the predominant and participated more than 90% of the total constituents (Figs. 2 and 3). Dolomite is noticed under microscope in scarce quantity with fine subhedral grains characterized by rhombohedral cleavage and symmetrical extinction, whereas it was undetectable by XRD due to its scarcity. Quartz has heterogeneous distribution wherever silicification has happened but, in general, existed in small quantities. Feldspar and gypsum are also existed as traces. Gypsum has scarce and heterogeneous distribution (Fig. 3).

Figure 4 illustrated the clay minerals as well as quartz and feldspar in a sample that has been treated with 10% HCl and 5% CH_3COOH acids for removing carbonates. Most of clay minerals are formed as a result of the physical and chemical weathering process which happened on various rocks during the digenetic processes or direct precipitation. Small quantities of kaolinite, montmorillonite, illite, and palygorskite are detected by XRD. Kaolinite primarily formed due to weathering of feldspars under acidic conditions. Palygorskite appear to be formed directly in shallow marine of alkali pH. This mineral requires alkaline conditions and high silicon and magnesium activities for stability (Singer 1989). Al-Bassam (2000) and Kadhim (2009) mentioned that this mineral formed in different environments range from marine to continental environments. Montmorillonite is very rare. The origin of illite is preferred to be potash feldspar. Illite is recognized by the weathering of silicates (primarily feldspar) through the alteration of other clay minerals.

Geochemistry

Table 2 displays the result of chemical analyses of cement raw materials which are compared with results of Duda 1985, who determined the acceptable limits of raw materials for cement industry.

Portland cement consists mainly of lime (CaO), silica (SiO_2), alumina (Al_2O_3), and ferric oxide (Fe_2O_3) compounds which constitute the bulk of the raw mix. The

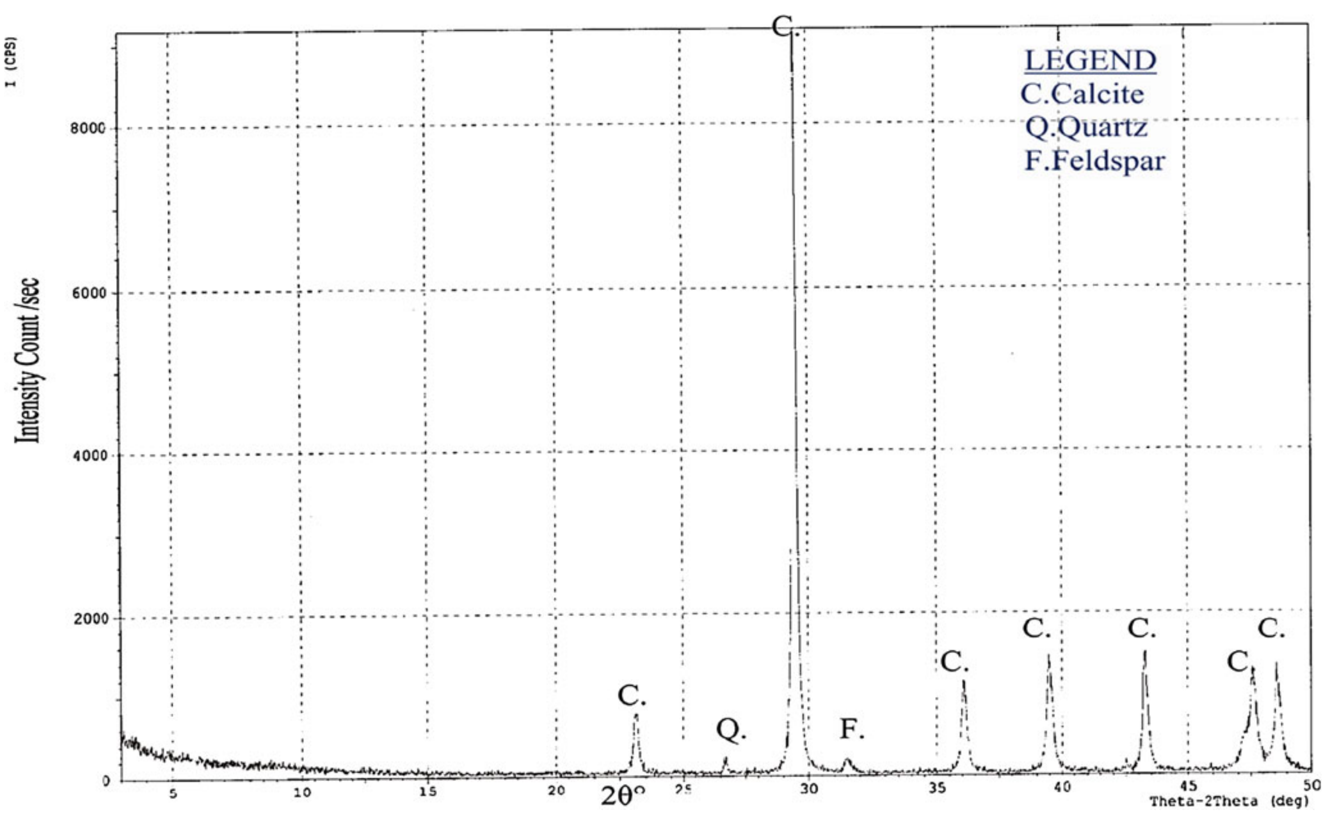

Fig. 2 X-ray diffractograph shows minerals in carbonate sample

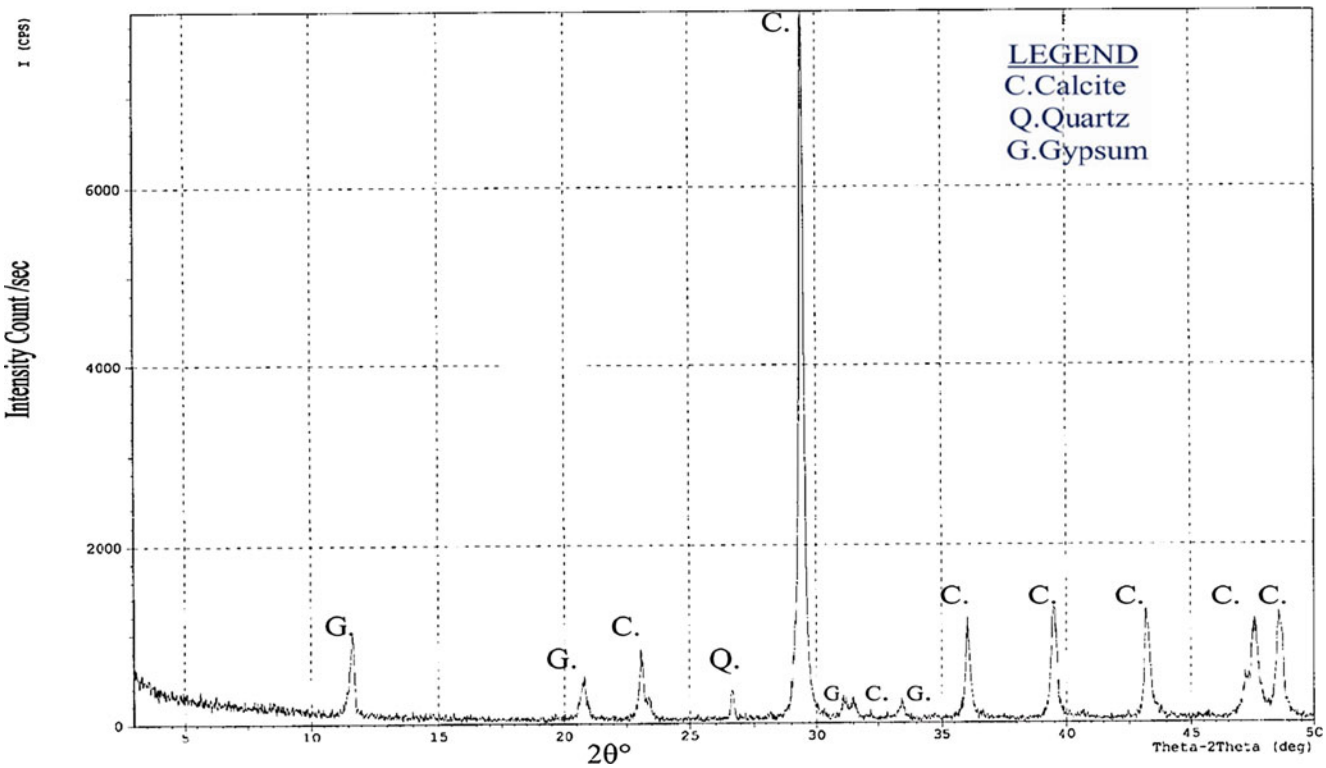

Fig. 3 X-ray diffractograph shows minerals in carbonate sample

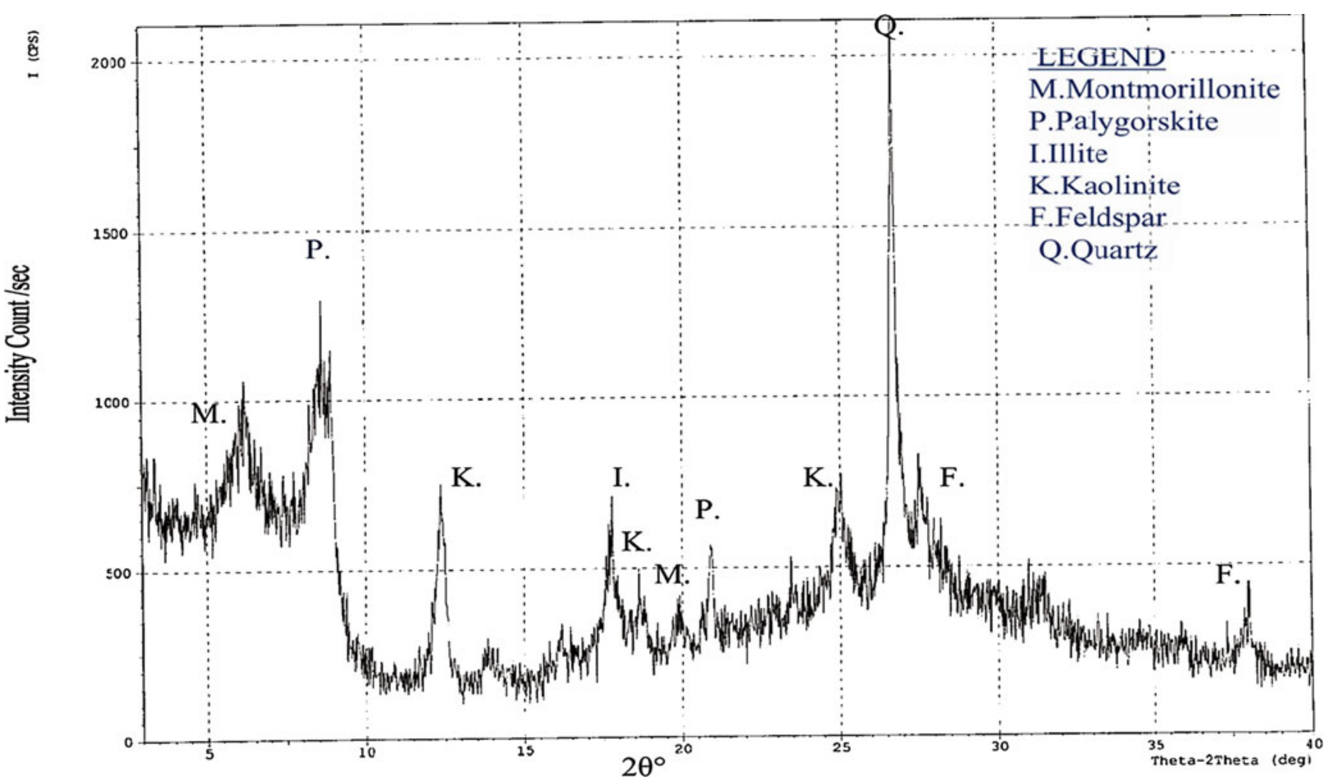

Fig. 4 X-ray diffractograph shows minerals treated with acids

Table 2 Results of chemical analyses of the Euphrates Formation raw materials

Well number	CaO%	MgO%	SO_3%	SiO_2%	Fe_2O_3%	Al_2O_3%	LOI%	Na_2O%	K_2O%	Cl%	Total%
1E	54.60	0.43	<.07	1.09	0.10	0.16	43. 39	0.05	0.03	0.10	99.95
2E	50.86	0.75	0.23	5.39	0.58	1.24	40.60	0.04	0.26	0.12	100.07
3E.	51.38	0.85	<.07	5.02	050	0.82	41.08	0.04	0.14	0.14	99.97
4E	45.40	1.50	0.27	10.42	1.36	3.86	36.0	0.13	0.35	0.14	99.43
5ED	54.30	0.47	<.07	1.21	0.19	0.32	43.08	0.20	0.03	0.18	99.03
6E	49.84	0.80	2.51	4.98	0.56	1.10	39.07	0.10	0.20	0.12	99.27
7E	54.42	0.49	0.32	3.29	0.10	0.17	40.93	0.09	0.04	0.09	99.94
8E	48.58	2.00	<.07	6.19	0.60	1.39	39.66	0.20	0.23	0.18	99.03
9ED	53.06	0.58	0.47	2.89	0.27	0.53	42.02	0.04	0.09	0.09	100.04
10E	54.60	0.48	<.07	0.90	0.22	0.43	42.98	0.06	0.08	0.09	99.84
11E	49.88	0.90	1.47	6.5	0.81	1.65	38.0	0.09	0.33	0.13	99.76
12E	47.28	1.15	0.26	8.7	1.12	2.39	38.11	0.07	0.52	0.12	99.72
13E	51.24	0.95	<.07	5.03	0.44	0.92	41.02	0.09	0.11	0.11	100.01
14ED	49.84	0.43	<.07	8.79	0.12	0.23	39.79	0.05	0.14	0.14	99.42
15E	54.78	0.37	0.57	0.71	0.08	0.14	43.05	0.04	0.02	0.14	99.9
16 E	49.1	1.0	<.07	6.5	1.06	1.27	39.9	0.05	0.15	0.12	99.15
17 ED	50.92	0.8	0.3	5.36	0.53	0.98	40.67	0.12	0.13	0.12	100.09
18 ED	52.36	0.75	<.07	3.67	0.19	0.53	41.83	0.03	0.03	0.12	99.51
19 ED	53.9	0.65	<.07	1.53	0.14	0.22	43.18	0.03	0.02	0.09	99.76
20 ED	52.12	1.50	2.1	1.9	0.42	0.97	40.69	0.06	0.04	0.09	99.89
21 ED	52.82	0.65	2.09	2.41	0.13	0.20	41.02	0.16	0.03	0.11	99.62
Range	45.4–54.7	0.37–2.0	<.07–2.5	0.71–10.42	0.10–1.36	0.14–3.86	35.66–43.39	0.03–0.20	0.02–0.35	0.09–0.18	99.03–100.09
Average	51.40	0.83	0.52	4.3	0.45	0.93	40.72	0.08	0.14	0.1	99.70
Duda 1985	≥45.0	≤2.0	≤1.5	≤6.75	≤0.66	≤2.0	≥38.0	≤0.28	≤0.2	≤0.1	

combined content of these four oxides (major constituents) is approximately 90% of the cement weight. The remaining (minor constituents) 10% consists of magnesia (MgO), alkalis (Na_2O and K_2O), chloride (Cl^-), and SO_3. A few percent of gypsum usually added during grinding for regulating the setting time of the cement (Lea 1970; Soroka 1979; Kohlhaas 1983; Duda 1985).

The concentration of CaO ranges from 45.5% to 54.7% with an average of 51.5%. LOI produced by decomposition of carbonate minerals as CO_2, ranges from 35.6% to 43.4% with an average of 40.7%. The domination of calcite with lack of dolomite reflected in the content of the MgO which ranged from 0.37% to 2.0% with average of (0.83%).

Silica (SiO_2) and alumina (Al_2O_3) are originated from clay mineral suites but part of silica also belongs to quartz. SiO_2 ranges from 0.71% to 10.42% with an average 4.3%. Sometime silica exists as lenses in some of the studied samples as in well 4E in depth 5 m. Al_2O_3 ranges from 0.14% to 3.86% with average 0.93% are derived totally from clay minerals.

Fe_2O_3 ranges from 0.1% to 1.36% with an average 0.52%; some of ferrous (Fe^{2+}) could replace Mg^{2+} in dolomite (Rankama and Sahama 1950). In addition to dolomite, this oxide may be originated from many sources such as clay minerals and limestone even these exist as traces.

SO_3 participated in less quantity of the total LOI; it is ranged from 0.07% to 2.5% with average 0.52%. It is yielded from gypsum lenses that are presence within the Euphrates Formation. Sulfur content in the final product of cement may be higher. Generally, the sulfur source in the produced cement attributed to the raw materials, the added gypsum to the clinker, and the used water in clinker mixture as well as the used fuel (black oil). Duda (1977) and Schafer (1987) mentioned that the sulfur content in cement belongs to the raw materials and the used fuel.

Alkalis appear to have low content; Na_2O ranges from 0.03% to 0.2% with average of 0.08%, whereas K_2O ranges from 0.02% to 0.35% with average of 0.14%.

Chloride (Cl^-) may be originated from the ground water or from halite during evaporation of sea water; it ranges from 0.09% to 0.18% with average of 0.1%. Major oxides and minor constituents appear to be qualified for cement industry in comparison with standard results of Duda 1985.

Reserve estimation

The number of drilled wells is a control factor for estimating the reserve where provides us with subsurface imaginary picture. The study area which is extended on 2×2 km^2 has penetrated with 21 wells (Fig. 1). Correlation of mineralogical and geochemical data of these wells is done in order to estimate the bed extension. Stratigraphic correlation revealed that the gypseous soil, marl, clayey limestone, and conglomeratic limestone are extending as discontinues beds and lenses (non-industrial beds), embedded within the limestone industrial beds as shown in (Figs. 5 and 6). To compute the reserve of limestone as cement raw material accurately, subtraction of the non-industrial bed from reserve calculation became recom-

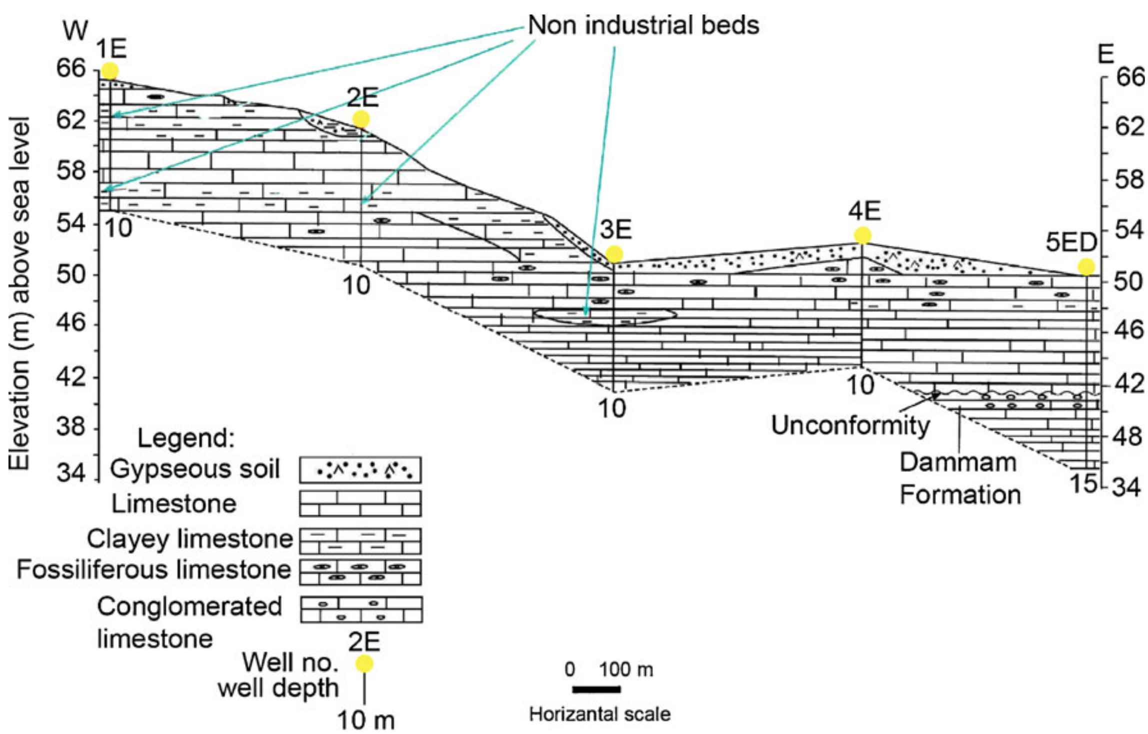

Fig. 5 Geological cross-section shows industrial bed and non-industrial bed of east–west-ward across five wells (1E to 5ED)

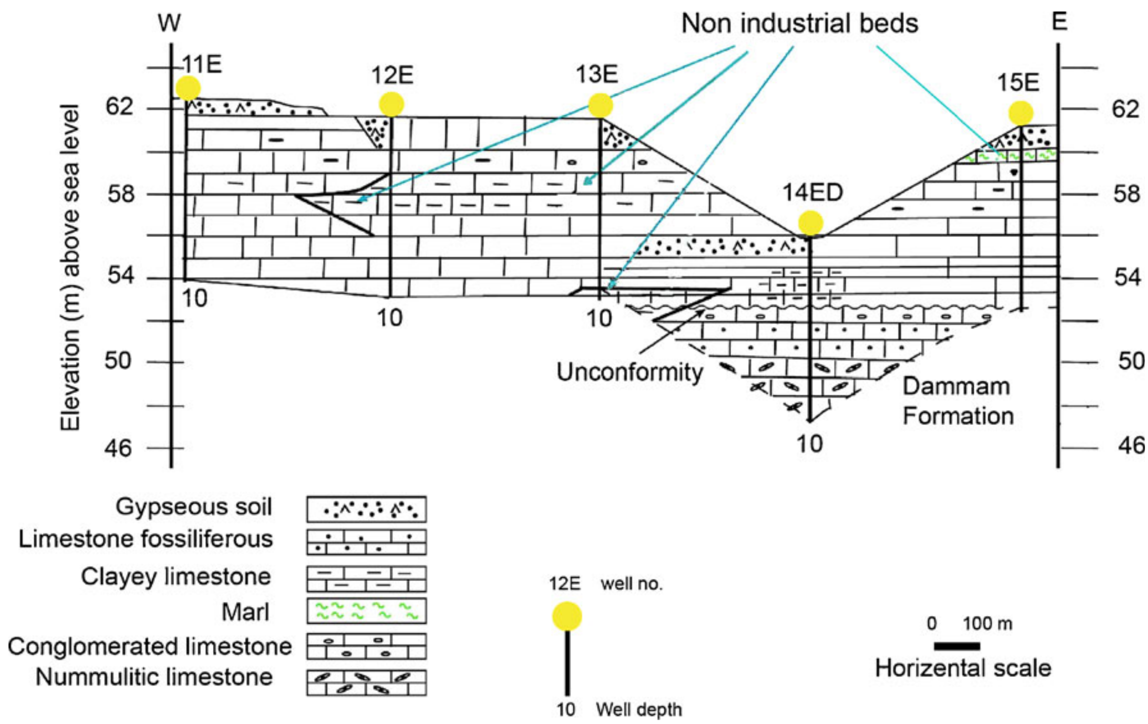

Fig. 6 Geological cross-section shows the non-industrial bed emplacing within the industrial bed across five wells (11E to 15E)

Table 3 The thickness averages of overburden, industrial, and non-industrial beds

Well no.	Overburden thickness (m)	Industrial bed thickness (m)	Non-industrial bed thickness (m)
1E	0.7	6.3	3.0
2E	0.9	7.1	2.0
3E	0.25	7.0	2.75
4E	1.6	7.1	1.3
5ED	0.5	14.5	–
6E	0.8	5.6	3.6
7E	0.9	6.9	2.2
8E	0.5	6.3	3.2
9ED	0.7	9.3	–
10E	0.3	8.9	0.8
11E	1.4	8.6	–
12E	0.7	6.3	3.0
13E	0.7	6.7	2.6
14ED	0.2	8.3	1.5
15E	1.0	8.0	1.0
16E	0.75	8.0	1.25
17ED	0.8	7.6	1.6
18ED	0.9	9.1	–
19ED	0.1	12.0	2.9
20ED	0.3	6.6	3.1
21ED	2.0	11.0	2.0
Range	0.1–1.6	5.6–14.5	0.8–3.6
Average	0.76	8.15	1.80

mended. The thickness of each of overburden, industrial bed, and non-industrial bed is measured during digging processes. Overburden thickness ranges between 0.1 and 1.6 m with average 0.76 m (Table 3; Fig. 7). Thickness of the industrial bed ranges between 5.6 m at the well 6E and 14.5 m at the well 5ED with average 8.15 m (Table 3; Fig. 8). Thickness of non-industrial bed ranged between 0.8 and 3.6 m with average 1.8 m (Table 3) which is canceled from limestone reserve estimation. Physical properties (bulk density and compressive strength) are measured in ten samples selected from ten wells (Table 4). The bulk density is used for estimating the reserve volume. The compressive strength is used for classifying the rock hardness which is considered as medium-tough.

The stripping index which is an arithmetic ratio between volume of the overburden and volume of the industrial bed (Al-Atia 2001) is applied as follows:

$$\mathrm{SI} = \mathrm{OV}/\mathrm{IV}$$

Where:

SI is the stripping index
OV is the volume of the overburden bed (m^3)
IV is the volume of the industrial bed (m^3).

$$\mathrm{OV} = A \times \mathrm{TO}$$

A is the total area which equals 2,000×2,000= 4,000,000 m^2.
TO is an average thickness of the overburden.

$$\mathrm{OV} = 4{,}000{,}000\,\mathrm{m}^2 \times 0.76\,\mathrm{m} = 3{,}040{,}000\,\mathrm{m}^3$$

$$\mathrm{IV} = A \times \mathrm{TI}$$

TI is the average thickness of industrial bed.

$$\mathrm{IV} = 4{,}000{,}000\,\mathrm{m}^2 \times 8.15\,\mathrm{m} = 32{,}600{,}000\,\mathrm{m}^3$$

$$\mathrm{SI} = 3040000\,\mathrm{m}^3/32600000\,\mathrm{m}^3 = 0.1$$

Many methods could be used for reserve estimation, but, in case of the current study, the Triangle Block Method is

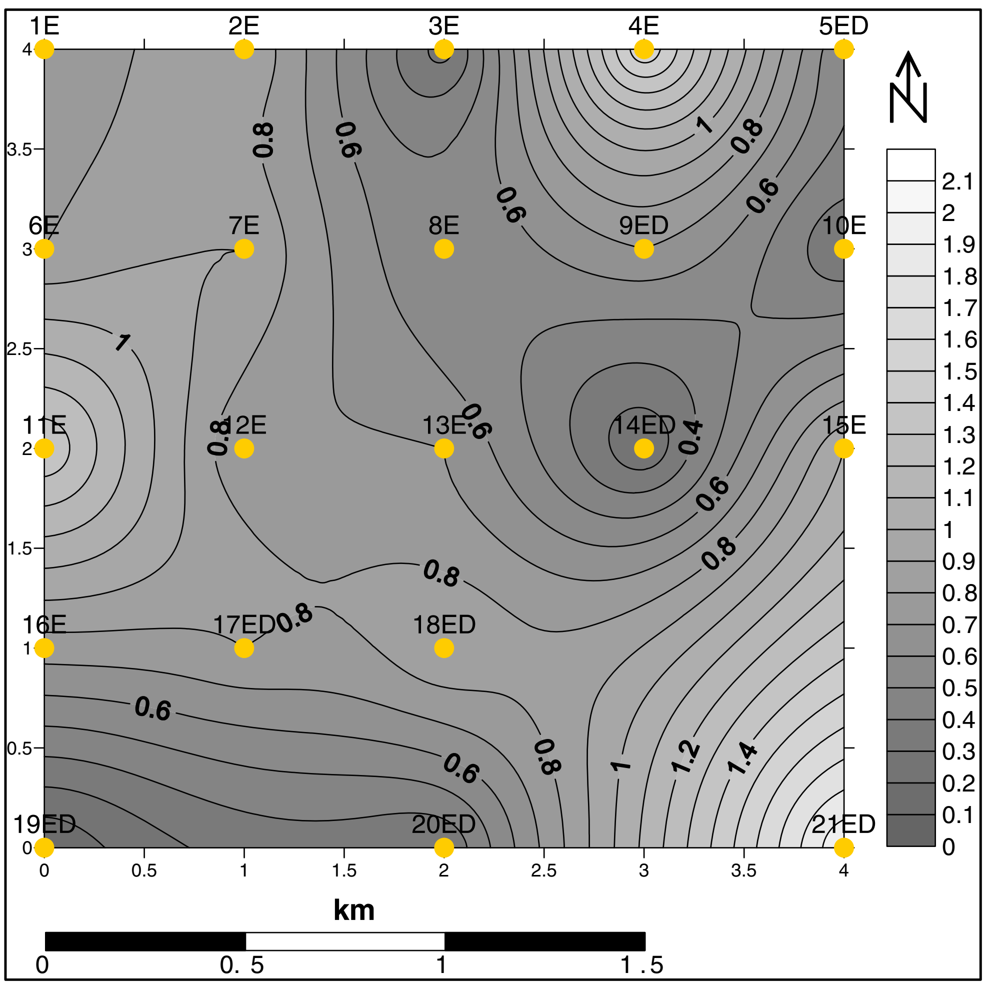

Fig. 7 Isopach map displays the distribution of the overburden thickness

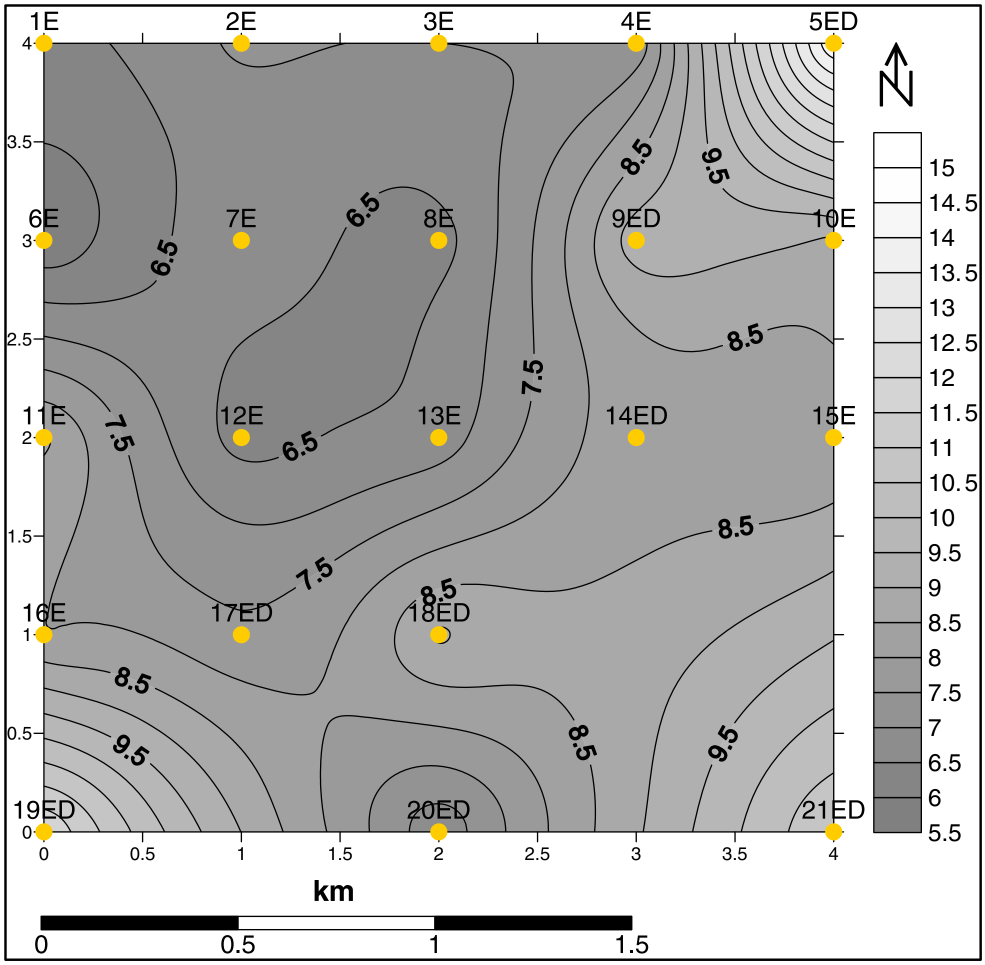

Fig. 8 Isopach map displays the distribution of the industrial bed thickness

preferable. Accordingly, it is chosen and applied to calculate the reserve of limestone. Square area has 2× 2 km^2 is divided into 25 triangles (Fig. 9), where each triangle represents three wells. Because of the unequal sides of the triangle, the correction factor is recommended and applied (Table 5).

$$\text{Correction factor (C.F.)} = \text{Angle of the triangle peak}/60$$

Table 4 Bulk density and compressive strength of selected samples

Well number	Sample number	Interval depth (m)		Thickness of sample core (m)	Bulk density (g/cm³)	Compressive strength (mega N/m²)
		From	To			
3E	1	5.20	5.40	0.20	1.87	4.9
5ED	2	7.80	7.90	0.10	2.4	23.4
6E	3	6.40	6.50	0.10	2.2	48.24
8E	4	5.60	5.70	0.10	1.90	0.3
11E	5	2.40	2.50	0.10	1.66	27.56
15E	6	3.00	3.20	0.20	1.94	0.23
16E	7	1.00	1.10	0.10	1.65	0.22
18ED	8	7.60	7.70	0.10	2.5	23.2
19ED	9	6.80	6.90	0.10	2.5	23.9
20ED	10	1.50	1.65	0.15	1.78	41.35
Average					2.04	19.3

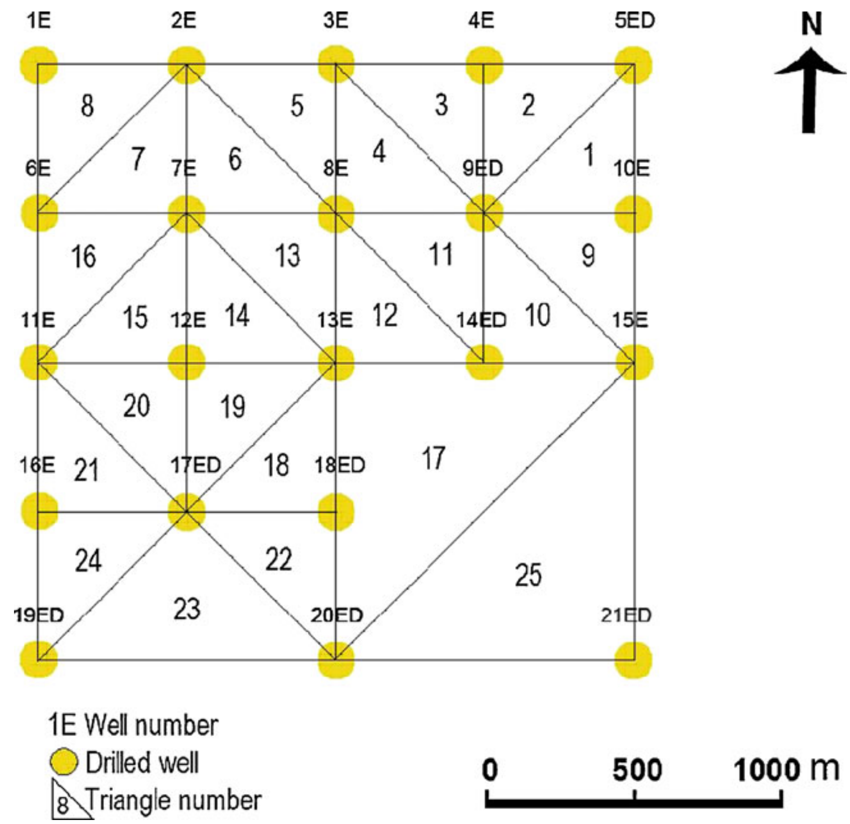

Fig. 9 Network of the Triangle Block method of the study area

Table 5 Calculations of reserve estimation by using the Triangle Block method

Triangle number	Well number	Thickness of bed (T), m	Correction factor (CF)	CT (T×CF)	Average CT (A×CT)	Area, m²	BD, Gm/cm³	Reserve (ACT×A×BD), ton
1	10E	8.9	90/60=1.5	13.35	10.39	125,000	2.04	2,649,450
	9 ED	9.3	45/60=0.75	6.97				
	5ED	14.5	45/60=0.75	10.87				
2	4E	7.1	90/60=1.5	10.65	9.49	125,000	2.04	2,419,950
	5ED	14.5	45/60=0.75	10.87				
	9ED	9.3	45/60=0.75	6.97				
3	4E	7.1	90/60=1.5	10.65	7.62	125,000	2.04	1,943,100
	9ED	9.3	45/60=0.75	6.97				
	3E	7.0	45/60=0.75	5.25				
4	8E	6.3	90/60=1.5	9.45	7.22	125,000	2.04	1,841,100
	9ED	9.3	45/60=0.75	6.97				
	3E	7.0	45/60=0.75	5.25				
5	3E	7.0	90/60=1.5	10.5	6.84	125,000	2.04	1,744,200
	8E	6.3	45/60=0.75	4.72				
	2E	7.1	45/60=0.75	5.32				
6	7E	6.9	90/60=1.5	10.35	6.79	125,000	2.04	1,731,450
	8E	6.3	45/60=0.75	4.72				
	2E	7.1	45/60=0.75	5.32				
7	7E	6.9	90/60=1.5	10.35	6.62	125,000	2.04	1,688,100
	6E	5.6	45/60=0.75	4.20				
	2E	7.1	45/60=0.75	5.32				
8	1E	6.3	90/60=1.5	9.45	6.32	125,000	2.04	1,611,600
	6E	5.6	45/60=0.75	4.20				
	2E	7.1	45/60=0.75	5.32				
9	10E	8.9	90/60=1.5	8.9×1.5	8.02	125,000	2.04	2,045,100

Table 5 (continued)

Triangle number	Well number	Thickness of bed (T), m	Correction factor (CF)	CT (T×CF)	Average CT (A×CT)	Area, m²	BD, Gm/cm^3	Reserve (ACT×A×BD), ton
	8E	6.3	45/60=0.75	4.72				
	15E	8.0	45/60=0.75	6.0				
10	14ED	8.3	90/60=1.5	12.45	8.47	125000	2.04	2,159,850
	15E	8.0	45/60=0.75	6.0				
	9ED	9.3	45/60=0.75	6.97				
11	9ED	9.3	90/60=1.5	13.95	8.29	125,000	2.04	2,113,950
	14ED	8.3	45/60=0.75	6.22				
	8E	6.3	45/60=0.75	4.72				
12	13E	6.7	90/60=1.5	10.05	6.99	125,000	2.04	1,782,450
	14ED	8.3	45/60=0.75	6.22				
	8E	6.3	45/60=0.75	4.72				
13	8E	6.3	90/60=1.5	9.45	6.54	125,000	2.04	1,667,700
	13E	6.7	45/60=0.75	5.02				
	7E	6.9	45/60=0.75	5.17				
14	12E	6.3	90/60=1.5	6.54	6.54	125,000	2.04	1,667,700
	13E	6.7	45/60=0.75	5.02				
	7E	6.9	45/60=0.75	5.17				
15	12E	6.3	90/60=1.5	9.45	7.02	125,000	2.04	1,790,100
	11E	8.6	45/60=0.75	6.45				
	7E	6.9	45/60=0.75	5.17				
16	6E	5.6	90/60=1.5	8.4	6.67	125,000	2.04	1,700,850
	11E	8.6	45/60=0.75	6.45				
	7E	6.9	45/60=0.75	5.17				
17	13E	6.7	90/60=1.5	10.05	7.0	500,000	2.04	7,140,000
	20ED	6.6	45/60=0.75	4.95				
	15E	8.0	45/60=0.75	6.0				
18	18ED	9.1	90/60=1.5	13.65	8.12	125,000	2.04	2,070,600
	17ED	7.6	45/60=0.75	5.7				
	13E	6.7	45/60=0.75	5.02				
19	12ED	6.3	90/60=1.5	9.45	6.72	125,000	2.04	1,713,600
	17ED	7.6	45/60=0.75	5.7				
	13E	6.7	45/60=0.75	5.02				
20	12ED	6.3	90/60=1.5	9.45	7.20	125,000	2.04	1,836,000
	17ED	7.6	45/60=0.75	5.7				
	11E	8.6	45/60=0.75	6.45				
21	16E	8.0	90/60=1.5	12.0	8.05	125,000	2.04	2,052,750
	17ED	7.6	45/60=0.75	5.7				
	11E	8.6	45/60=0.75	6.45				
22	18ED	9.1	90/60=1.5	13.65	6.54	125,000	2.04	1,667,700
	17ED	7.6	45/60=0.75	5.7				
	20ED	6.6	45/60=0.75	4.95				
23	17ED	7.6	90/60=1.5	11.4	8.45	250,000	2.04	4,309,500
	17ED	7.6	45/60=0.75	5.7				
	19ED	12.0	45/60=0.75	9.0				
24	16E	8.0	90/60=1.5	12.0	8.90	125,000	2.04	2,269,500
	17ED	7.6	45/60=0.75	5.7				
	19ED	12.0	45/60=0.75	9.0				
25	21ED	11.0	90/60=1.5	16.5	9.15	500,000	2.04	9,333,000
	20ED	6.6	45/60=0.75	4.95				
	15ED	8.0	45/60=0.75	6.0				
Total								63 million tons

T thickness, *CF* correction factor, *CT* corrected thickness, *BD* bulk density

Conclusions

Mineral constituents participated in supplying the necessary oxides that are used as cement raw materials. The average of chemical composition of limestone of the Euphrates Formation: CaO (51.5), MgO (0.83), SO_3 (0.54), SiO_2 (4.3), Fe_2O_3 (0.45), Al_2O_3 (0.93), L.O.I (40.7), Na_2O_3 (0.08), K_2O (0.14), and Cl^- (0.1) proved that the limestone is within the standard limits for cement raw materials and appears to be qualified for cement industry according to Duda 1985. Sixty-three million tons are determined and expressed as a new potential quarry, according to the British system classification; this reserve could be classified as a probable reserve which will be a supplying source for the limestone raw material for both Al-Najaf and Al-Kufa cement plants. This reserve will be sufficient for the next 25 years for operating the Al-Najaf and Al-Kufa cement plants according to the current designed capacities. The rock hardness is medium-tough according to the scale of rock hardness. During digging processes, the water table of ground water appears to be under the bottom of the Euphrates Formation. Mining conditions (rock hardness, topography, and ground water) are suitable for mining.

References

Al-Atia MJ (2001) Evaluation of Mineral Deposits, Practices in Economic Geology. GEOSURV, Iraq, 157P

Al-Bassam KS (2000) The Iraqi Palygorskite: Geology, Mineralogy, Geochemistry, Genesis and Industrial Uses. GEOSURV, Baghdad, 237P

Al-Hashimi HA (1973) The sedimentary facies and depositional environment of the Eocene Dammam and Rus formations, J. Geol. Soc. Iraq; 6:1–18

Al-Hashimi HA, Amer RM (1985) Tertiary Microfacies of Iraq. Geological Survey and Mineral Investigation, Baghdad, 56P

Al-Sayyab A, Al-Ansari N, Al-Rawi D, Al-Jassim JA, Al-Omari F, Al-Sheikh Z (1982) Geology of Iraq. Mosul University Printing, Mosul, Iraq, 277

Barwary AM and Naseira AS (1995) The Geology of Al-Najaf Quadrangle, State Establishment of Geological Survey and Mining (Internal Report) pp 20–23

Buday T (1980) The Regional Geology of Iraq. Stratigraphy and Paleogeography Publication of GEOSURV, Baghdad, 1:445

Cytroky P and Karim S A (1971) Stratigraphy and Paleontology of the Oligocene and Miocene strata near Anah, Euphrates Valley. NIMCO Report No. CZ 140, SOM Library, Baghdad.

Dawood RM (2000) Mineralogy, origin of celestite and the factors controlling its distribution in Tar Al-Najaf, Najaf Plateau. Msc. Thesis, Baghdad University, Iraq.

Dabous AA, Awadalla H, El-Kammer AM, Selim SR (1989) Geochemical specification of some lower tertiary limestones and shales from Upper- Egypt as raw materials for Portland cement industry. Alexandria University, Egypt, pp 313–325

Duda WH (1977) “Cement-Data-Book” International Process Engineering in the Cement Industry, 2nd edn. Bauveriag, GmbH, Wiesbaden and Berlin, 539P

Duda WH (1985) “Cement-Data-Book” International Process Engineering in the Cement Industry, 3rd edn. Bauveriag, GmbH, Wiesbaden and Berlin, 636P

Jassim SZ, Goff JC (eds) (2006) Geology of Iraq. Dolin, Prague and Moravian Museum, Brno, p 341

Kadhim MA (2009) Geochemistry and mineralogy of palygorskite-rich clays in Gercus Formation in Dohuk governorate, north of Iraq. M. Sc. Thesis, University of Baghdad, 115 P.

Kohlhaas B (1983) Cement Engineer’s Handbook 4th English ed. Bauverlag GMBH, Wiesbaden and Berlin, p 800

Lea FM (1970) The Chemistry of Cement and Concrete, 3rd edn. Chemical Publishing Company, Inc., New York, NY, p 727

Rankama K, Sahama TG (1950) Geochemistry Report No. 2496. University of Chicago. Chicago, IL, Baghdad, p 912

Schafer HU (1987) Assessment of raw materials for the industry, reprinted from the journal “World Cement” no.7, pp 273–283, Cement and Concrete Association, London.

Singer A (1989) Palygorskite and Sepiolite Group Minerals. In: Dixon JB, Weed SB (eds) Minerals in soil environment, 2nd edn. Soil Science Society of America, Madison, WI, pp 829–872

Sissakian V-Kh (1999) The Nfayil Formation. GEOSURV Internal Report, Baghdad, Iraq

Soroka I (1979) Portland cement paste and concrete. MacMillan Press Ltd., London, UK p, 338